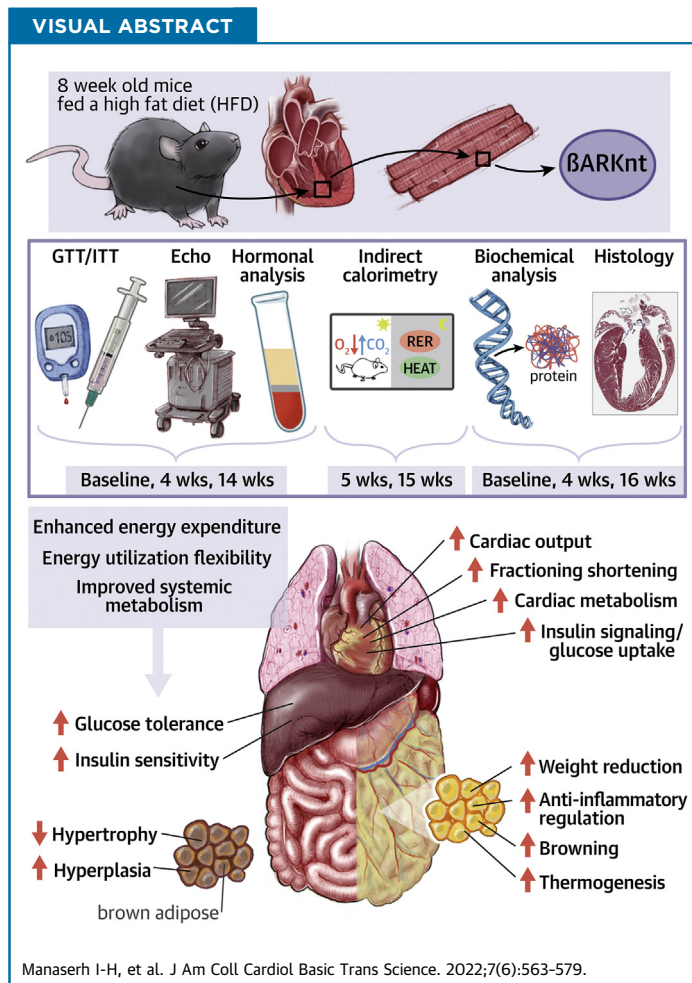


PRECLINICAL RESEARCH

A Cardiac Amino-Terminal GRK2 Peptide Inhibits Maladaptive Adipocyte Hypertrophy and Insulin Resistance During Diet-Induced Obesity



Iyad H. Manaserh, PhD, Kamila M. Bledzka, PhD, Alex Junker, MPH, Jessica Grondolsky, Sarah M. Schumacher, PhD



HIGHLIGHTS

- Heart disease remains the leading cause of death, in part due to increasing diabetes and obesity, though the exact mechanisms linking these disorders are not fully understood.
- In a diet-induced obesity model, we found that cardiac expression of an amino-terminal peptide of GRK2, β ARKnt, preserves systemic glucose tolerance and insulin sensitivity despite normal weight gain.
- β ARKnt enhanced metabolic flexibility, increased energy expenditure, protected against maladaptive visceral adipocyte hypertrophy, and induced visceral fat browning.
- β ARKnt further elicited cardioprotection and increased insulin-mediated AS160 signaling during metabolic stress.
- These data point to a noncanonical cardiac regulation of systemic metabolic homeostasis that may lead to new treatment modalities for metabolic syndrome.

From the Department of Cardiovascular & Metabolic Sciences, Lerner Research Institute, Cleveland Clinic, Cleveland, Ohio, USA. The authors attest they are in compliance with human studies committees and animal welfare regulations of the authors' institutions and Food and Drug Administration guidelines, including patient consent where appropriate. For more information, visit the [Author Center](#).

Manuscript received August 9, 2021; revised manuscript received January 13, 2022, accepted January 13, 2022.

**ABBREVIATIONS
AND ACRONYMS** **β ARKct** = cardiac restricted expression of C-terminus domain of GRK2 **β ARKnt** = cardiac-restricted expression of N-terminus domain of GRK2**AS160** = Akt substrate of 160 kilodaltons**BAT** = brown adipose tissue**GRK2** = G protein-coupled receptor kinase 2**gWAT** = gonadal white adipose tissue**HFD** = high-fat diet**HOMA-IR** = homeostatic model assessment of insulin resistance**mTOR** = mechanistic target of rapamycin protein kinase**NLC** = nontransgenic littermate control**NP** = natriuretic peptide**NPR** = natriuretic peptide receptor**RER** = respiratory exchange ratio**T2D** = type II diabetes**Tg** = transgenic**SUMMARY**

Heart disease remains the leading cause of death, and mortality rates positively correlate with the presence of obesity and diabetes. Despite the correlation between cardiac and metabolic dysregulation, the mechanistic pathway(s) of interorgan crosstalk still remain undefined. This study reveals that cardiac-restricted expression of an amino-terminal peptide of GRK2 (β ARKnt) preserves systemic and cardiac insulin responsiveness, and protects against adipocyte maladaptive hypertrophy in a diet-induced obesity model. These data suggest a cardiac-driven mechanism to ameliorate maladaptive cardiac remodeling and improve systemic metabolic homeostasis that may lead to new treatment modalities for cardioprotection in obesity and obesity-related metabolic syndromes. (J Am Coll Cardiol Basic Trans Science 2022;7:563-579) © 2022 The Authors. Published by Elsevier on behalf of the American College of Cardiology Foundation. This is an open access article under the CC BY-NC-ND license (<http://creativecommons.org/licenses/by-nc-nd/4.0/>).

Heat disease is the leading cause of death in the United States, and these mortality rates positively correlate with the presence of diabetes and obesity.^{1,2} Independent of sex, age, and developmental status of the country, the worldwide prevalence of obesity and severe obesity (body mass index ≥ 35 kg/m²) continues to progress with severe adverse effects on cardiovascular risk factors including plasma glucose and lipids, arterial blood pressure, inflammation, and cardiorespiratory fitness.^{3,4} Further, obesity is causally linked to adverse changes in cardiac structure and function, including left ventricular hypertrophy, left atrial enlargement, and altered systolic and diastolic function, thereby increasing the incidence of congestive heart disease, atrial fibrillation, and heart failure.^{3,4} In response to the structural and cellular remodeling of the adipose tissue to accommodate the excessive caloric intake, adipocyte-derived cytokine (adipokine) release is dysregulated,⁵ and adipocyte death and tissue inflammation are enhanced, leading to increased circulating fatty acids and lipotoxicity risk, and insulin resistance.^{5,6} Metabolic disruptions such as insulin resistance, a hallmark of type II diabetes (T2D), also contribute to the poor prognosis of heart failure.^{7,8} Further, the injured and remodeling heart secretes a variety of inflammatory cytokines and metabolic and lipid mediators that can impact the function of peripheral organs including the kidneys, adipose tissue, or liver, thereby aggravating the detrimental cycle among the heart and key metabolic tissues.^{9,10} In the midst of a growing recognition of the effect of adipose tissue dysfunction and adipokine imbalance on cardiovascular disease in the obese population, a less-well understood mechanism is that of the effect of cardiac metabolism and function on whole-body metabolic

homeostasis. The idea that the heart produces signals (cardiokines/myokines) that can change distant organ function has been gaining recognition over the past several years,¹¹⁻¹³ supporting the concept of endocrine interactions between the heart and metabolically active tissues. Moving forward, identification of factors linking dysfunction in cardiac and systemic metabolism, and a more comprehensive understanding of systemic metabolic activity, is imperative for the development of therapeutic interventions for cardiometabolic diseases.

Though the exact mechanisms linking cardiac function and metabolic homeostasis have yet to be elucidated, G protein-coupled receptor (GPCR) kinase 2 (GRK2) is known to play a crucial regulatory role.^{14,15} Neurohormonal up-regulation of GRK2 occurs in conjunction with cardiac stress,¹⁶⁻¹⁸ resulting in the desensitization of β -adrenergic receptors (β ARs) and subsequent loss of contractile reserve that leads to heart failure.^{8,15,17,18} Additionally, GRK2 is an active modulator of whole-body metabolism through mechanisms underlying insulin signaling,¹⁹ brown adipose tissue (BAT) thermogenesis,²⁰ and adiposity.^{20,21} Investigation of GRK2 functional domain interactions involved in cardiac and metabolic regulation could advance understanding of their coordination and aid in the development of treatments that benefit both simultaneously.

GRK2, also known as β ARK1, consists of 3 functional domains: the amino-terminus, central catalytic domain, and carboxyl-terminus.^{22,23} Overexpression of the catalytic domain negatively affects cardiac function, whereas overexpression of either the carboxyl-terminus (β ARKct, a competitive inhibitor of GRK2) or N-terminus (β ARKrgs) is cardioprotective.²² Recent studies have also shown that overexpression of full-length GRK2 in response to cardiac injury down-regulates fatty acid uptake in the heart, whereas overexpression of β ARKct enhances fatty

structure and function, including left ventricular hypertrophy, left atrial enlargement, and altered systolic and diastolic function, thereby increasing the incidence of congestive heart disease, atrial fibrillation, and heart failure.^{3,4} In response to the structural and cellular remodeling of the adipose tissue to accommodate the excessive caloric intake, adipocyte-derived cytokine (adipokine) release is dysregulated,⁵ and adipocyte death and tissue inflammation are enhanced, leading to increased circulating fatty acids and lipotoxicity risk, and insulin resistance.^{5,6} Metabolic disruptions such as insulin resistance, a hallmark of type II diabetes (T2D), also contribute to the poor prognosis of heart failure.^{7,8} Further, the injured and remodeling heart secretes a variety of inflammatory cytokines and metabolic and lipid mediators that can impact the function of peripheral organs including the kidneys, adipose tissue, or liver, thereby aggravating the detrimental cycle among the heart and key metabolic tissues.^{9,10} In the midst of a growing recognition of the effect of adipose tissue dysfunction and adipokine imbalance on cardiovascular disease in the obese population, a less-well understood mechanism is that of the effect of cardiac metabolism and function on whole-body metabolic

acid uptake.¹⁵ Our group has recently found that mice overexpressing a short peptide of the amino-terminus, β ARKnt, exhibit baseline hypertrophy, a normal adaptive response to transaortic constriction, and yet cardioprotection during chronic pressure overload.²³ Interestingly, these studies uncovered a significant increase in cardiomyocyte insulin and Akt substrate of 160 kDa (AS160) signaling in the β ARKnt mice, in contrast to endogenous GRK2, which is known to phosphorylate insulin receptor substrate 1 (IRS-1) and negatively regulate insulin signaling in the heart.⁸ This increase in insulin and AS160 signaling led to enhanced cardiomyocyte ATP production and spare respiratory capacity in the presence of both glucose and the fatty acid substrate palmitate.²³ Further, these β ARKnt mice exhibited a decrease in gonadal white adipose tissue (gWAT) weight, equivalent to human abdominal fat, both at baseline and 4 weeks after cardiac stress.²³ In the present study, we subjected these cardiac-specific β ARKnt transgenic (Tg) male mice to high fat diet (HFD) stress to investigate the linkage between these beneficial cardiac and metabolic effects and determine whether they might prove cardioprotective during metabolic dysfunction. Our data indicate beneficial effects on both cardiac remodeling and systemic metabolism after HFD and support the idea that the β ARKnt peptide is not only cardioprotective during cardiac stress, but also demonstrates a novel means of cardioprotection and cardiac-mediated regulation of obesity and systemic metabolism during metabolic stress.

METHODS

For a detailed Methods section, see the Appendix. All animal procedures were carried out according to National Institutes of Health Guidelines on the Use of Laboratory Animals and approved by the Animal Care and Use Committees of the Lerner Research Institute. The method of euthanasia is consistent with the American Veterinary Medical Association Guidelines for the Euthanasia of Animals. Euthanasia was accomplished by intraperitoneal injection of a single dose of ketamine/xylazine (87.5-100/10-12.5 mg/kg body weight) followed by blood collection, thoracotomy, and heart excision.

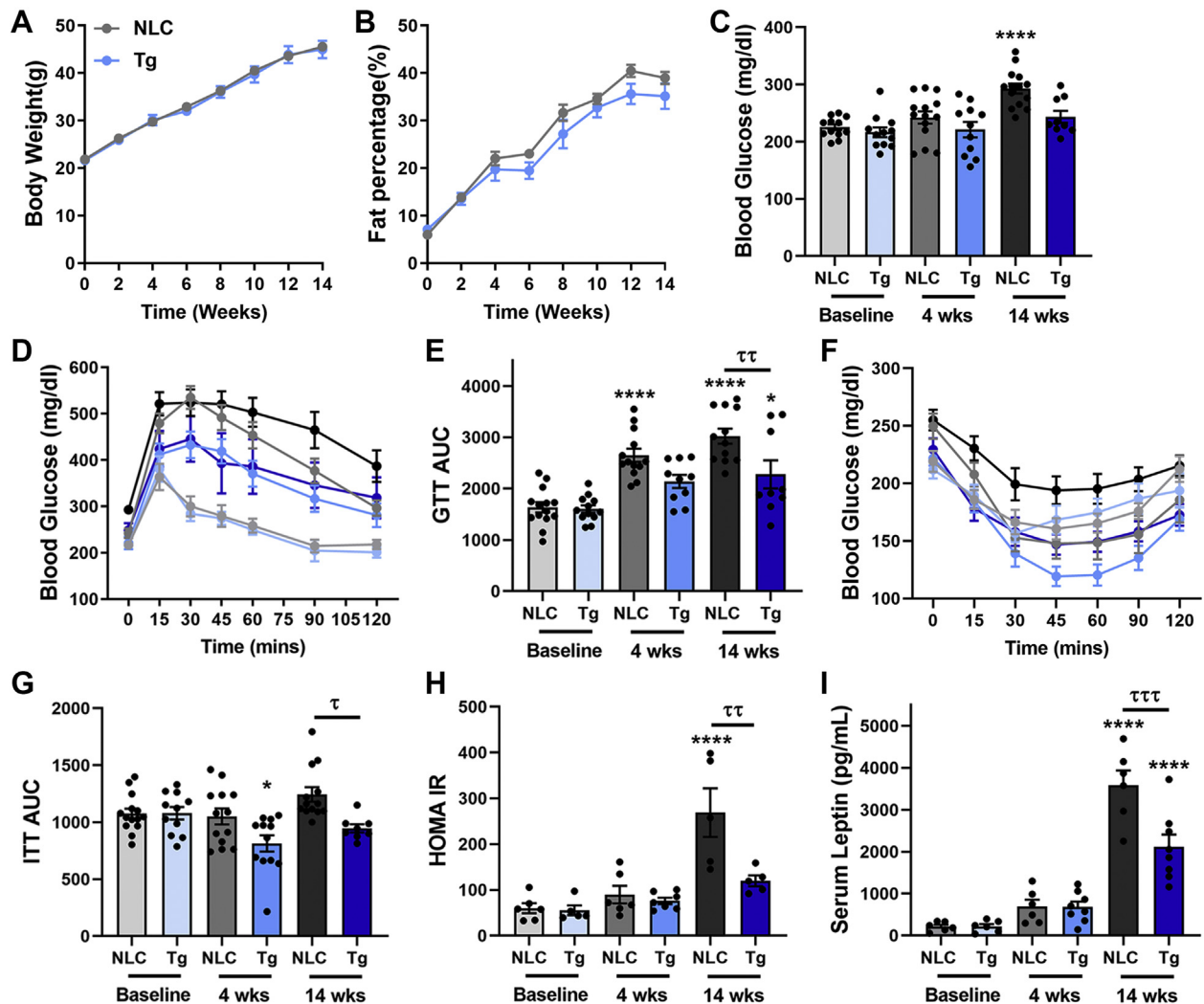
STATISTICAL ANALYSIS. All values in the text and figures are presented as mean \pm SEM of independent experiments for given size N. Statistical significance was determined by 1-way analysis of variance with repeated measures (where appropriate and as indicated) and Tukey's post hoc test for multiple pairwise comparisons, or 2-way analysis of variance with

repeated measures and Bonferroni's post hoc test for comparisons at a given time point. For all statistical tests, a *P* value of <0.05 was considered significant. Analyses were performed using GraphPad Prism 9 software (GraphPad Software).

RESULTS

Tg β ARKnt MICE EXHIBIT IMPROVED SYSTEMIC METABOLISM DESPITE EQUIVALENT BODY COMPOSITION CHANGES AFTER HFD FEEDING.

To examine the effect of cardiomyocyte-specific β ARKnt expression on cardiac function and metabolism in the presence of metabolic stress, 8-week-old male Tg β ARKnt and non-Tg littermate control (NLC) mice were enrolled in a 16-week HFD study ([Supplemental Figure S1](#)). The HFD-fed C57BL/6J mouse model, introduced by Surwit et al in 1988,²⁴ is a widely used experimental animal model of food-induced obesity and its relevant symptoms such as hyperlipidemia, hyperglycemia, insulin resistance, T2D, and low-grade inflammation.^{25,26} Using this model, we observed no overall difference in body weight gain between the NLC and β ARKnt mice over time ([Figure 1A](#)), and analysis with an EchoMRI device revealed no difference in the corresponding increase in fat percentage ([Figure 1B](#)) or decrease in lean mass ([Supplemental Figure S2A](#)) in these animals. Of note, this is not consistent with gain or loss of function of full-length GRK2, wherein inhibition of GRK2's canonical GPCR activity by β ARKct has been shown to induce an obesogenic phenotype with enhanced weight gain, whereas overexpression of GRK2 induces an overall lean phenotype with reduced weight gain after HFD feeding.²⁷ Interestingly, though, in contrast to the significant increase in fasting blood glucose in control mice after 14 weeks of HFD, this value remained near baseline measures in the β ARKnt mice ([Figure 1C](#)), despite this equivalent weight gain. These results suggest improved glucose clearance from the bloodstream in Tg mice compared with control mice. To further measure the response to blood glucose and assess insulin sensitivity, we performed both glucose tolerance tests and insulin tolerance tests on these animals at baseline, and 4 and 14 weeks of HFD stress. Whereas blood glucose levels were comparable before HFD, β ARKnt mice exhibited a trend toward enhanced glucose tolerance at 4 weeks that is significant compared with the glucose-intolerant NLC mice at 14 weeks of HFD ([Figures 1D and 1E](#)). Further, in contrast to the NLC mice that develop insulin resistance, insulin sensitivity is preserved in the β ARKnt mice at 4 and 14 weeks ([Figures 1F and 1G](#)). Because total weight gain and fat percentage are

FIGURE 1 Glucose Tolerance, and Insulin and Leptin Sensitivity in Tg β ARKnt Mice After HFD Stress

Despite a comparable increase in body weight and fat percentage, Tg β ARKnt mice exhibit improved glucose tolerance, and enhanced insulin and leptin sensitivity after high-fat diet (HFD) stress. **(A)** Body weight (BW) and **(B)** fat percentage in nontransgenic littermate control (NLC) and transgenic (Tg) β ARKnt mice at baseline, and 2 to 14 weeks after HFD ($n = 12-14$ per group). **(C)** Blood glucose levels before intraperitoneal (IP) injection ($n = 9-14$ per group). **(D)** Glucose tolerance test (GTT) measurements of blood glucose levels after IP injection of 2 g/kg per BW of a sterile dextrose solution. **(E)** Area under curve (AUC) measurements of GTT ($n = 10-14$ per group). **(F)** Insulin tolerance test (ITT) measurements of blood glucose levels after IP insulin injection of 0.75 U/kg per BW recombinant human insulin. **(G)** AUC measurements of ITT ($n = 10-14$ per group). **(H)** Homeostatic assessment model of insulin resistance (HOMA-IR) score ($n = 5-7$ per group). **(I)** Quantification of serum leptin levels from these mice ($n = 6-8$ per group). * $P < 0.05$; **** $P < 0.0001$ by 1-way ANOVA with repeated measures and Tukey post hoc test relative to corresponding NLC baseline. † $P < 0.05$; †† $P < 0.01$; ††† $P < 0.001$ by 1-way ANOVA with repeated measures and Tukey post hoc test relative to corresponding NLC 4 or 14 weeks post-HFD. ANOVA = analysis of variance.

comparable between groups, these data demonstrate that the improved glucose uptake and insulin sensitivity in the β ARKnt mice is not an indirect effect of reduced obesity.

Fasting blood glucose and serum insulin levels (Supplemental Figure S2B) were then used to perform the homeostatic model assessment of insulin

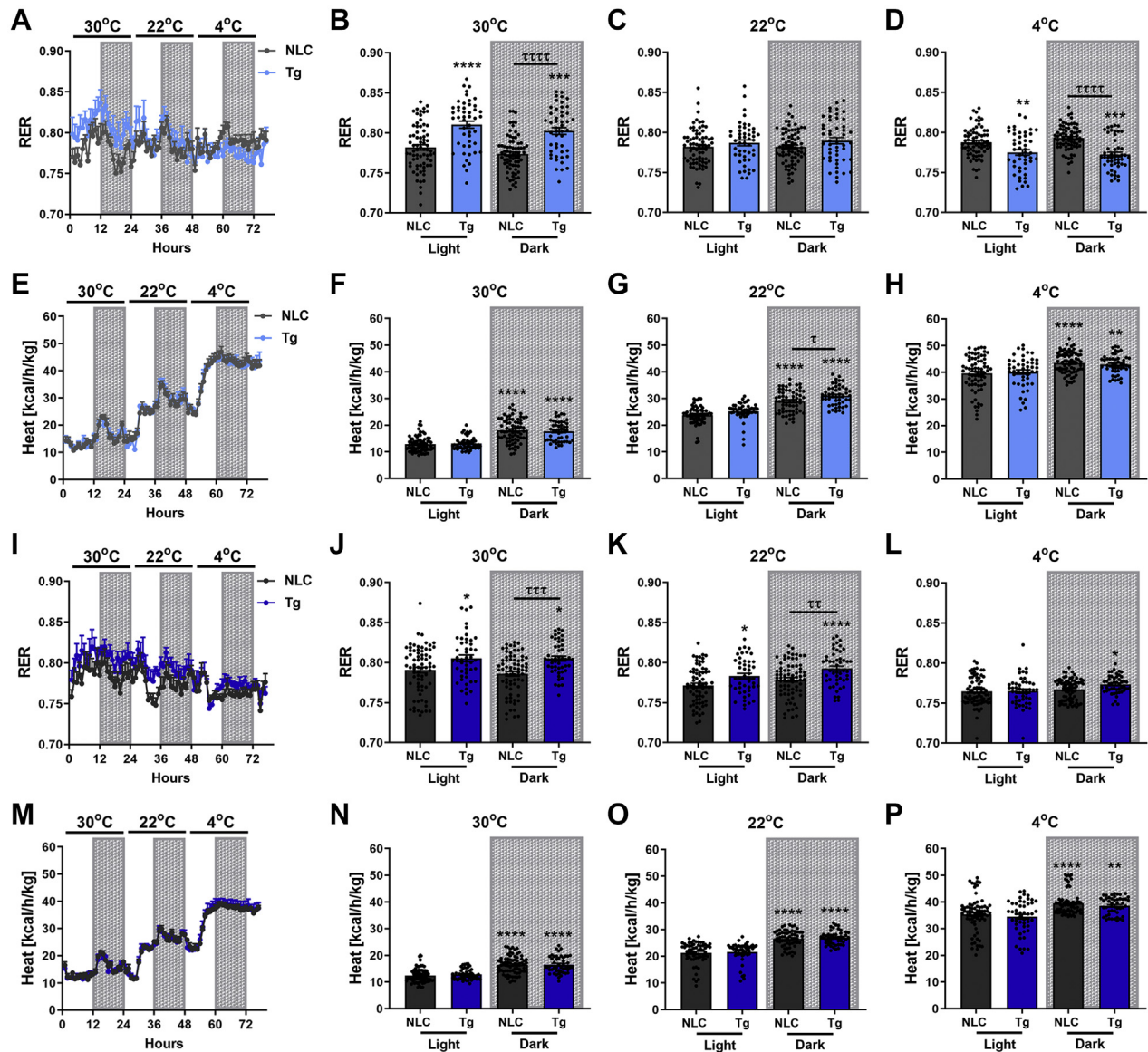
resistance (HOMA-IR) calculation (Figure 1H). Together, these blood glucose, glucose tolerance test, serum insulin, and HOMA-IR data confirm that although control mice become insulin resistant, glucose tolerance and insulin sensitivity are significantly improved in the β ARKnt mice after 14 weeks of chronic HFD. Further serum analysis using mesoscale

Uplex and Rplex assays revealed dramatically elevated serum leptin levels in control mice that were significantly reduced by cardiac β ARKnt expression after chronic HFD exposure (Figure 1I). Recent clinical studies have revealed that insulin or leptin resistance evaluated by HOMA-IR score and serum leptin levels, respectively, were good indicators for cardiovascular disease risk.²⁸ Thus, the reduction in HOMA-IR score and serum leptin levels after 14 weeks of HFD in the β ARKnt mice not only indicate improved systemic metabolic performance, but also suggest protection from metabolic dysfunction-induced cardiac risk. Relevant differences were not observed for other peptide hormone regulators of metabolism such as adiponectin (Supplemental Figure S2C), glucagon like peptide-1 (GLP-1) (Supplemental Figure S2D), or glucagon (Supplemental Figure S2E). Together, these data demonstrate that despite equivalent weight gain, cardiac β ARKnt expression elicits a beneficial effect on systemic insulin responsiveness and metabolic hormone signaling during HFD-induced metabolic stress. This suggests that β ARKnt may induce expression of a beneficial cardiokine or other heart-mediated systemic cross-talk to metabolically active tissues.

β ARKnt MICE DEMONSTRATE METABOLIC FLEXIBILITY AND ENHANCED ENERGY EXPENDITURE FOLLOWING HFD STRESS. To further elucidate the effect of cardiomyocyte β ARKnt on systemic metabolic performance, we performed indirect calorimetry measures of energy utilization and expenditure in these NLC and Tg mice at 5 and 15 weeks after HFD. Weight gain, in addition to hyperglycemia and hyperinsulinemia in mice, drives insulin resistance and negatively alters energy balance through decreases in energy expenditure, physical activity, and/or respiratory exchange, all of which can be readily evaluated through indirect calorimetry measures in metabolic cages.^{3,4} The ratio of carbon dioxide produced over oxygen consumed as measured in expired air provides the respiratory exchange ratio (RER). Normally, this ratio falls between a value of 0.7 and 1.0, wherein a reading near 0.7 indicates the mice are primarily using fatty acid metabolites for energy production, whereas a reading near 1.0 suggests carbohydrate usage.^{29,30} At 5 and 15 weeks after HFD, both the NLC and β ARKnt mice showed comparable O_2 consumption (V_{O_2}) (Supplemental Figures S3A to S3H) and CO_2 production (VC_{O_2}) (Supplemental Figures S3I to S3P) at a normothermic condition (30°C) and room temperature (22°C), as well as during cold challenge (4°C). Interestingly, the RER was significantly different between groups (Figure 2A), wherein it was significantly

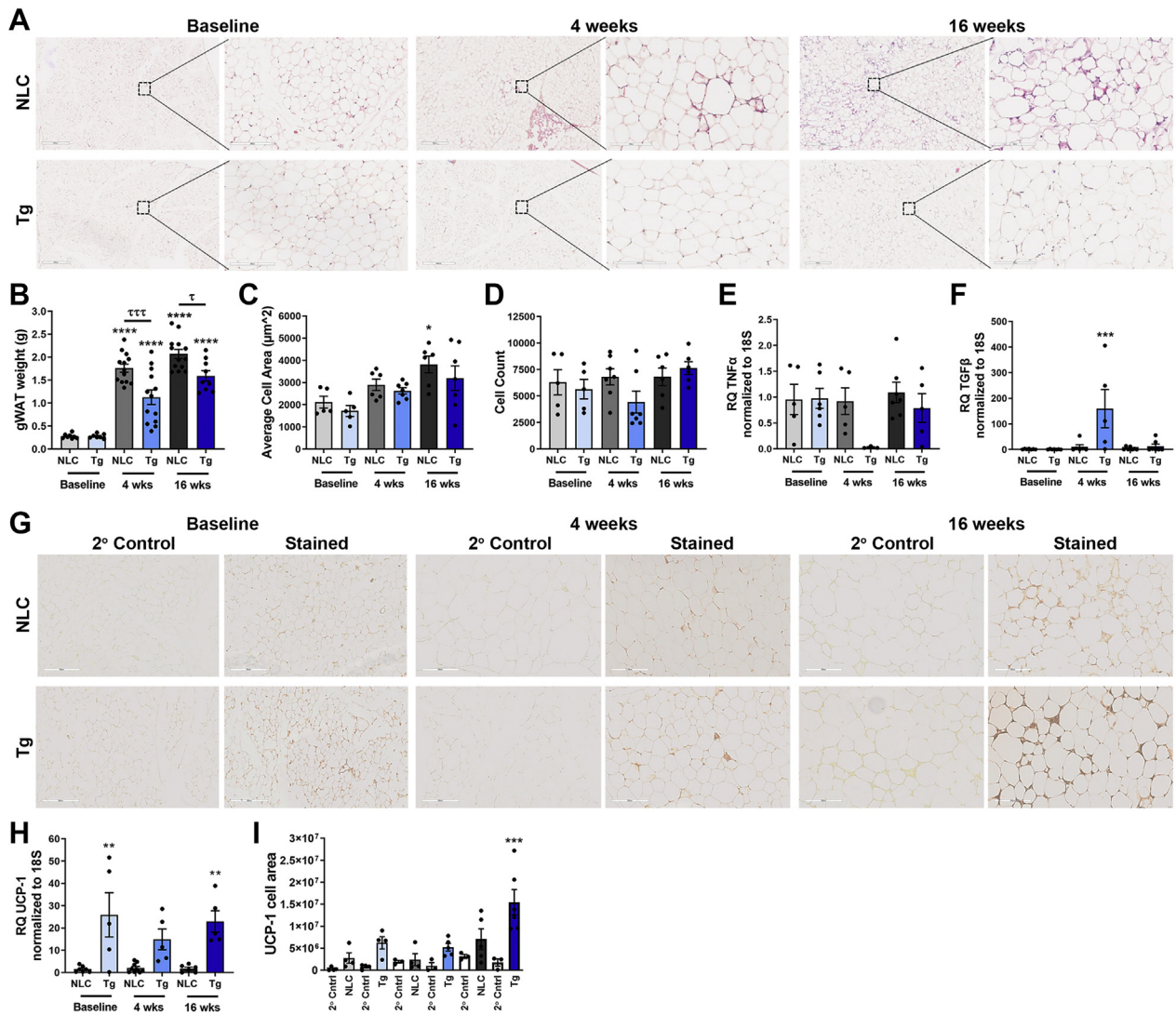
elevated during the normothermic condition (Figure 2B), unchanged at room temperature (Figure 2C), and reduced during cold challenge (Figure 2D) in both the light and dark cycles in the β ARKnt compared with control mice after 5 weeks of HFD stress. These data suggest decreased utilization of lipids for energy expenditure during normothermic conditions versus increased lipid usage during cold challenge in the β ARKnt mice, suggesting more metabolic flexibility. As expected, measures of heat production increased with decreasing environmental temperatures in both groups, as well as during the dark versus light phases. Notably, β ARKnt mice displayed enhanced heat production (energy expenditure) compared with NLC mice at 22°C (Figures 2E and 2G), with comparable levels at 30°C (Figure 2F) or 4°C (Figure 2H), indicating enhanced thermogenesis as early as 5 weeks after HFD stress. Following chronic HFD stress (15 weeks post-HFD), β ARKnt mice burn less fat than NLC mice at 30°C (Figures 2I and 2J) and 22°C (Figure 2K), with no differences at 4°C (Figure 2L) and comparable heat production between groups (Figures 2M to 2P). Of note, ambulatory locomotor activity was no different between the β ARKnt and NLC mice at 5 or 15 weeks after HFD, indicating that differences in basal activity levels are not influencing the major endpoints of this study (Supplemental Figure S4). Together, these data demonstrate a more flexible state in lipid utilization that may counter adipose and systemic dysfunction.

β ARKnt MICE EXHIBIT REDUCED ABDOMINAL FAT WITH AN IMPROVED INFLAMMATORY AND ENERGETIC PHENOTYPE AFTER HFD STRESS. To understand this metabolic flexibility and increased energy expenditure in the β ARKnt mice, we examined the health of the gWAT. In the lean state, healthy fat is well-vascularized with minimal immune cell infiltration and releases numerous anti-inflammatory adipokines.³¹ During chronic overnutrition, adipocytes first expand in size by hypertrophy, and when they reach threshold, continue to expand in number by hyperplasia (adipogenesis).³² Excessive hypertrophic adipocyte enlargement leads to adipocyte death and tissue inflammation with crowning of dead adipocytes by macrophages, vascular rarefaction, proinflammatory adipokine release that generates systemic inflammatory activation, increased circulating fatty acids and lipotoxicity risk, and insulin resistance.^{5,6} Histological analysis of gWAT by hematoxylin and eosin staining revealed an expected increase in adipocyte size in both the NLC and Tg β ARKnt mice from baseline to 4 and 16 weeks of HFD, but with a visually observable decrease in adipocyte crowning in

FIGURE 2 Fat Utilization and Heat Production in Tg β ARKnt Mice After HFD Stress

Tg β ARKnt mice demonstrate metabolic flexibility in utilizing fat and increased heat production (energy expenditure) following HFD stress. Mice were fed ad libitum and subjected to indirect calorimetry analysis to assess light and darkness cycle of (A) Respiratory exchange ratio (RER) in NLC and Tg β ARKnt mice after 5 weeks of HFD. Values represent measurements of 3 consecutive days ($n = 4-6$ per group). Quantitative measurements of RER in these mice at (B) 30°C, (C) room temperature (22°C), and (D) 4°C. (E) Heat production in NLC and Tg β ARKnt mice after 5 weeks of HFD. Values represent measurements of 3 consecutive days ($n = 4-6$ per group). Quantitative measurements of heat production in these mice at (F) 30°C, (G) room temperature (22°C), and (H) 4°C. (I) RER in NLC and Tg β ARKnt mice after 15 weeks of HFD. Values represent measurements of 3 consecutive days ($n = 4-6$ per group). Quantitative measurements of RER in these mice at (J) 30°C, (K) room temperature (22°C), and (L) 4°C. (M) Heat production in NLC and Tg β ARKnt mice after 15 weeks of HFD. Values represent measurements of 3 consecutive days ($n = 4-6$ per group). Quantitative measurements of heat production in these mice at (N) 30°C, (O) room temperature (22°C), and (P) 4°C. * $P < 0.05$; ** $P < 0.01$; *** $P < 0.001$; **** $P < 0.0001$ by 1-way ANOVA with repeated measures and Tukey post hoc test relative to corresponding NLC light phase at 5 or 15 weeks. † $P < 0.05$; †† $P < 0.01$; ††† $P < 0.001$; †††† $P < 0.0001$ by 1-way ANOVA with repeated measures and Tukey post hoc test relative to corresponding NLC dark phase at 5 or 15 weeks post-HFD. Abbreviations as in Figure 1.

FIGURE 3 gWAT Weight, Molecular Markers of Anti-Inflammation, and Browning in Tg β ARKnt Mice Before and After HFD Stress



Tg β ARKnt mice exhibit a reduction in gonadal white adipose tissue weight, increased molecular markers of anti-inflammation, and enhanced browning before and after HFD stress. **(A)** Representative images of hematoxylin and eosin-stained gonadal white adipose tissues (gWAT) from NLC and Tg β ARKnt mice at baseline, 4 weeks and 16 weeks after HFD (scale bar: 500 μ m [left], 200 μ m [right]; magnification: 5 \times [left], 20 \times [right]). **(B)** gWAT weight at baseline, and 4 and 16 weeks after HFD (n = 7-14 per group). Quantification of **(C)** average cell area, and **(D)** cell count in these mice at baseline, and 4 and 16 weeks after HFD (n = 5-7 per group). Quantification of reverse transcription polymerase chain reaction (RT-PCR) data in gWAT in these mice showing fold change (RQ = $2^{-\Delta\Delta C_t}$) in mRNA expression of **(E)** TNF α and **(F)** TGF β (n = 5-9 per group). **(G)** Representative images of UCP-1-stained gonadal white adipose tissues (gWAT) from NLC and Tg β ARKnt mice at baseline, and 4 weeks and 16 weeks after HFD (scale bar: 200 μ m; magnification: 15 \times). Quantification of RT-PCR data in gWAT in these mice showing fold change (RQ = $2^{-\Delta\Delta C_t}$) in mRNA expression of **(H)** UCP-1 markers (n = 5-9 per group). Quantification of **(I)** UCP-1 cell area in these mice at baseline, 4 and 16 weeks after HFD (n = 4-6 per group). $*P < 0.05$; $**P < 0.01$; $***P < 0.001$; $****P < 0.0001$ by 1-way ANOVA with repeated measures and Tukey post hoc test relative to corresponding NLC baseline. $\dagger P < 0.05$; $\dagger\dagger P < 0.001$ by 1-way ANOVA with repeated measures and Tukey post hoc test relative to corresponding NLC 4 or 16 weeks post-HFD. Abbreviations as in [Figure 1](#).

the β ARKnt tissues compared with control **(Figure 3A)**. Interestingly, and consistent with our pressure overload study,²³ gWAT weight was significantly reduced in the β ARKnt mice at 4 and 16 weeks

after HFD compared with control mice **(Figure 3B)**. Further, there was a coordinate decrease in average adipocyte size in these mice at 16 weeks compared with NLC **(Figure 3C)**, despite no overall difference in

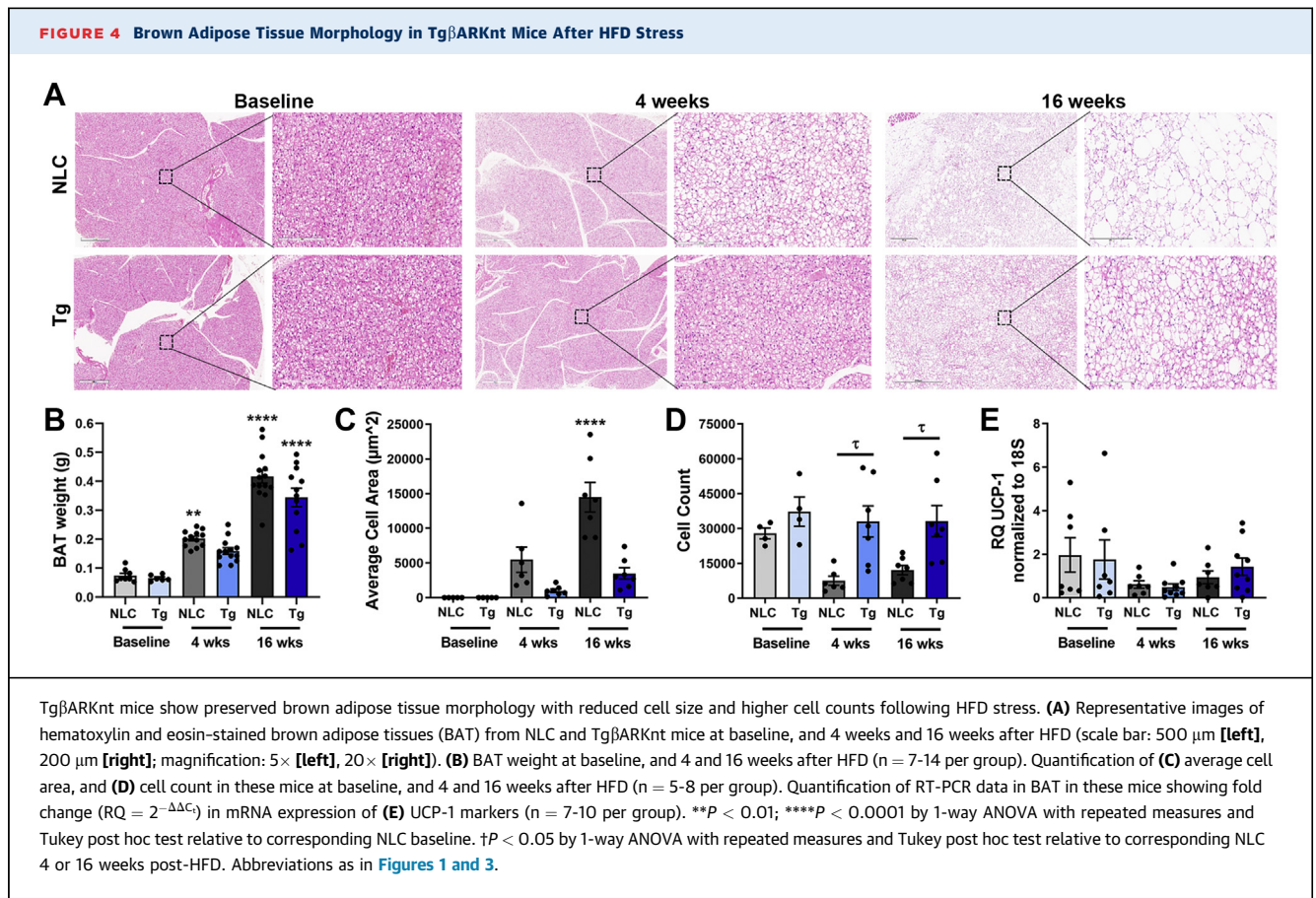
cell number between groups (Figure 3D). Reverse transcription polymerase chain reaction analysis of adipokine mRNA expression further revealed a significant decrease in proinflammatory tumor necrosis factor alpha (TNF α) (Figure 3E) and increase in anti-inflammatory transforming growth factor beta (TGF β) (Figure 3F) in Tg mice, though only at 4 weeks after HFD. Interestingly, we also observed a significant increase in serum IL-10 in both groups (Supplemental Figure S5A), though more robust in NLC, and coordinate with our mRNA results, a significant decrease in circulating TNF α levels in the β ARKnt mice compared with control mice at 16 weeks of HFD (Supplemental Figure S5B). Together, these data demonstrate maladaptive adipose tissue remodeling and dysfunction in control mice that is abrogated in mice with cardiomyocyte β ARKnt expression during acute and chronic HFD stress.

Under normal conditions, white fat acts mainly as a lipid storage depot. However, under certain conditions, it can undergo beiging to adopt a more brown adipose tissue-like phenotype.³³ During beiging, white adipocytes increase mitochondrial content and the energy expenditure marker mitochondrial uncoupling protein 1 (UCP-1) expression to utilize fatty acids for heat production, or thermogenesis. To determine whether the β ARKnt gWAT might be undergoing beiging, we performed immunohistochemical staining for UCP-1 protein expression in Tg and NLC gWAT at baseline, and 4 and 16 weeks after HFD feeding (Figure 3G). Coordinate reverse transcription polymerase chain reaction analysis revealed a significant increase in UCP-1 mRNA at baseline and 16 weeks, with a trend at 4 weeks, (Figure 3H), and this translated to a trend at baseline and 4 weeks, and significant increase in UCP-1 protein expression in the β ARKnt, but not NLC, gWAT at 16 weeks of HFD (Figure 3I). These data suggest an increase in gWAT beiging and thermogenic activity in mice with cardiomyocyte β ARKnt expression, consistent with the increased energy expenditure observed during our indirect calorimetry measures. Together, these data demonstrate that despite equivalent weight gain during chronic HFD stress, and characteristic maladaptive remodeling of the gWAT in NLC mice, β ARKnt mice exhibit reduced abdominal fat weight and adipocyte size, and increased markers of anti-inflammation and browning, suggesting a significantly improved gWAT phenotype following HFD stress.

β ARKnt MICE EXHIBIT A MORE PRESERVED BROWN FAT MORPHOLOGY AFTER HFD STRESS. In contrast to the lipid storage function of white fat, BAT is

saturated with mitochondria dedicated to producing heat through UCP-1-dependent uncoupled respiration of metabolites, thereby significantly modulating energy utilization and expenditure.³⁴ Because the β ARKnt mice exhibited metabolic flexibility under different temperature conditions and enhanced heat production after HFD stress, we investigated whether β ARKnt mice would demonstrate improved morphology and increased BAT UCP-1 expression. To determine whether the morphology of the subscapular BAT depots would be improved in the β ARKnt mice compared with control mice, we performed histological analysis of BAT by hematoxylin and eosin staining in Tg and NLC mice at baseline, and 4 and 16 weeks after HFD stress (Figure 4A). These data revealed a robust increase in lipid droplet storage within the BAT of NLC mice at 4 and 16 weeks after HFD, that was markedly restrained in the β ARKnt mice. Although overall BAT weight was no different between these groups (Figure 4B), average cell area was significantly increased only in control BAT at 16 weeks (Figure 4C), with a coordinate reduction in cell count per unit area in the NLC, compared with β ARKnt BAT (Figure 4D). No change in UCP-1 mRNA expression, or difference in anti- and proinflammatory markers, were observed over the time course of chronic HFD stress in these groups (Figure 4E, Supplemental Figure S6). Together, these data demonstrate that, in contrast to the significant lipid accumulation in NLC mice after chronic HFD, BAT morphology is improved in mice with cardiomyocyte β ARKnt expression. Interestingly, mRNA data indicate no overall change in tissue health or function between groups, suggesting that the increase energy expenditure observed in the β ARKnt mice during indirect calorimetry was not due to enhanced BAT activity, and must be due to other metabolically active tissues. Further studies will be needed to confirm that there is in fact no difference in BAT-mediated thermogenesis in the β ARKnt mice during chronic HFD stress.

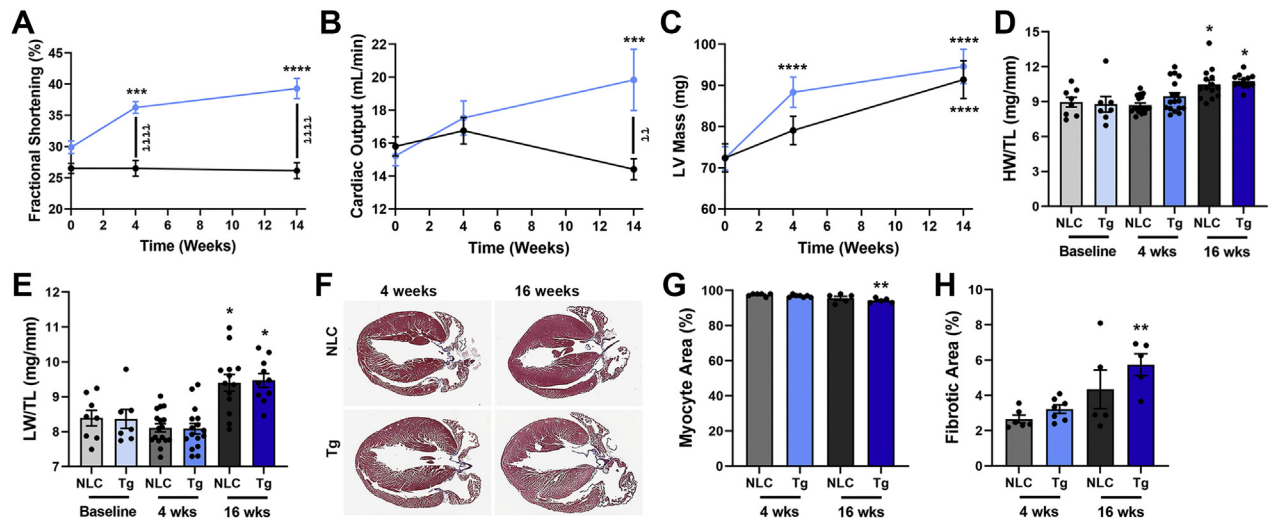
β ARKnt MICE EXHIBIT ENHANCED CARDIAC FUNCTION AND INSULIN-MEDIATED AS160 SIGNALING AFTER HFD STRESS. In response to diet-induced obesity, the heart initially undergoes adaptive remodeling, but cannot maintain this adaptive state and transitions into maladaptive remodeling, including pathological hypertrophy, fibrosis, and cardiac insulin resistance.^{23,35} To interrogate whether the enhanced systemic glucose tolerance and insulin sensitivity, and improved abdominal fat phenotype would correlate with preserved cardiovascular function, we performed echocardiographic analysis in these NLC and



Tg β ARKnt mice at baseline, and 4 and 14 weeks after HFD stress. In parallel to the role of cardiomyocyte β ARKnt in regulating systemic metabolism and energy expenditure, we observed enhanced cardiovascular performance. Echocardiography revealed a significant increase in fractional shortening in β ARKnt mice at 4 and 14 weeks after HFD, despite no overall change in control mice ([Figure 5A](#)). Further, cardiac output was significantly increased in β ARKnt compared with a trending decrease in NLC mice from 4 to 14 weeks after HFD ([Figure 5B](#)). Numerous other measures of cardiovascular structure and function were also enhanced in the Tg mice compared with control mice ([Table 1](#)), some of which have been previously shown to be affected by cardiomyocyte β ARKnt expression irrespective of metabolic stress.²³ Interestingly, although left ventricular mass was significantly increased in β ARKnt, but not NLC mice, at 4 weeks, this measure was equivalently elevated in both groups by 14 weeks ([Figure 5C](#)). This was accompanied by a comparable increase in heart weight ([Figure 5D](#), [Supplemental Figure S7A](#)) and

lung weight ([Figure 5E](#), [Supplemental Figure S7B](#)) in both groups after 16 weeks of chronic HFD stress. These data are accompanied by equivalent increases in both tibia length ([Supplemental Figure S7C](#)) and body weight ([Supplemental Figure S7D](#)) at 4 and 16 weeks of HFD feeding as expected for aging-related growth and HFD-induced weight gain, respectively.

To determine whether β ARKnt expression was able to reduce maladaptive left ventricular remodeling after chronic HFD stress, we performed Masson Trichrome staining of 4-chamber paraffin sections taken at the level of the aortic outflow tract. These images revealed a proportional increase in cardiac size in the NLC and Tg β ARKnt hearts from 4 to 16 weeks after HFD ([Figure 5F](#)). Quantification of ventricular myocyte and fibrotic area revealed no differences after acute HFD stress, but a significant decrease in myocyte area ([Figure 5G](#)) and increase in fibrotic area ([Figure 5H](#)) in the β ARKnt mice at after chronic metabolic stress. Although these differences are mild, an increase in fibrosis is generally considered at odds

FIGURE 5 Cardiac Function and Morphology in Tg β ARKnt Mice After HFD Stress

Despite enhanced hypertrophy, Tg β ARKnt hearts exhibit improved fractional shortening and cardiac output following HFD stress. Measures of (A) fractional shortening, (B) cardiac output, and (C) left ventricular (LV) mass from NLC and Tg β ARKnt mice at baseline, and 4 and 16 weeks after HFD ($n = 11-12$ per group). Measures of (D) heart weight (HW) normalized to tibia length (TL) (HW/TL), and (E) lung weight (LW) normalized to TL (LW/TL) from these mice ($n = 8-18$ per group). (F) Representative images of Masson trichrome-stained heart sections in these mice. Quantification of (G) myocyte area percentage, and (H) fibrotic area percentage from NLC and Tg β ARKnt hearts at 4 weeks and 16 weeks after HFD ($n = 5-7$ per group). * $P < 0.05$; ** $P < 0.01$; *** $P < 0.001$; **** $P < 0.0001$ by 2-way ANOVA with repeated measures and Tukey post hoc test relative to corresponding baseline (A to C), NLC baseline (D and E), or NLC 4 weeks (G and H). †† $P < 0.01$; †††† $P < 0.0001$ by 2-way ANOVA with repeated measures and Bonferroni post hoc test relative to corresponding NLC at 4 or 16 weeks post-HFD. Abbreviations as in Figure 1.

with an increase in cardiac output and stroke volume, and will require future investigation. Of note, the increase in fibrotic area (Figure 5H) and left ventricular posterior wall thickness during systole (Table 1), and decrease in end-systolic volume (Table 1) in the β ARKnt mice, indicates left ventricular hypertrophy and is consistent with our previous results during cardiac stress.²³

To investigate whether insulin-mediated AS160 signaling is similarly enhanced in β ARKnt-expressing cardiomyocytes as was observed in our previous pressure-overload study, we assessed insulin signaling via Western blot in ventricular lysates from NLC and Tg β ARKnt mice at 4 and 16 weeks after HFD stress. These studies revealed a significant increase in insulin receptor (InsR) protein expression levels in β ARKnt compared with NLC mice at 4 weeks, with only a trend at 16 weeks (Figure 6A, Supplemental Figures S8A and S9D). This led to a significant increase in downstream levels of phosphorylated Akt at 4 weeks (Figure 6B, Supplemental Figures S8B and S9A), with no difference in total Akt expression (Figure 6C, Supplemental Figures S8C and S9E). There was a similar increase in phosphorylated AS160 in the β ARKnt, but not NLC, mice at 4 weeks, with a further

significant increase at 16 weeks (Figure 6D, Supplemental Figure S8D), but no difference was observed in total AS160 protein levels (Figure 6E, Supplemental Figures S8E and S9B). This translated to a trend toward an increase at 4 weeks and significant increase at 16 weeks after HFD stress in downstream serine 2448 phosphorylation of mechanistic target of rapamycin protein kinase (mTOR), suggesting enhanced mTORC1 signaling in the β ARKnt lysates (Figure 6F, Supplemental Figure S8F) that was accompanied by a trend toward increased total mTOR (Figure 6G, Supplemental Figures S8G and S9C). These studies also revealed a coordinate increase in total glucose transporter 4 (GLUT4) protein expression in the β ARKnt mice compared with control mice after chronic HFD stress (Figure 6H, Supplemental Figure S8H). Together, these data suggest enhanced cardiac insulin signaling and glucose metabolism in the β ARKnt mice during metabolic stress that may underlie the observed increase in cardiovascular function.

NEITHER ENHANCED gWAT ACTIVATION NOR NATRIURETIC PEPTIDE ACTIVITY EXPLAINS THE IMPROVED gWAT PHENOTYPE AND SYSTEMIC METABOLISM OBSERVED IN THE β ARKnt MICE. To

elucidate the underlying mechanism(s) by which cardiomyocyte-specific β ARKnt expression enhances gWAT phenotype during metabolic stress, we further interrogated gWAT activation. Catecholamines act as prominent regulators of gWAT function, wherein by binding to β_3 -adrenergic receptors (β_3 ARs) they stimulate cAMP production and enhanced protein kinase A (PKA) activity, resulting in lipolysis and free fatty acid release.^{32,36} Therefore, we performed immunohistochemical staining for β_3 AR protein expression in the gWAT of NLC and Tg β ARKnt mice at baseline, and 4 and 16 weeks after HFD (Figure 7A). Quantification of these data revealed no significant difference in receptor expression between groups throughout the time course of the study (Figure 7B). Additionally, serum epinephrine levels showed no significant difference, and serum norepinephrine levels were equivalently enhanced over time in the β ARKnt and NLC mice in response to HFD stress (Figures 7C and 7D). Recent insights have shown that β_3 ARs and natriuretic peptides (NPs) share a common pathway for activation of gWAT and gWAT beiging.^{36,37} PKA and PKG, which are stimulated by β ARs and NP receptors (NPRs), respectively, share a closely related motif for substrate phosphorylation of mTOR to enhance mTORC1-mediated adipocyte browning.^{32,36}

The atrial (ANP) and B-type (BNP) endocrine-like NPs are normally produced by atrial myocytes; however, their expression in ventricular myocytes is significantly enhanced in response to cardiovascular and cardiometabolic stress. NP stimulation of NP receptor A (NPRA) activates adipocyte browning through mTORC1 signaling,^{32,38} whereas NP receptor C (NPRC) acts as a clearance receptor involved in NP degradation.^{39,40} Therefore, the ratio of NPRA:NPRC determines NP signaling capacity in abdominal fat. ANP (Figure 7E) and NPRC (Figure 7G) mRNA levels were comparable between groups; however, β ARKnt mice exhibited increased NPRA gene expression after 4 weeks of HFD stress (Figure 7F). This resulted in a significant increase in the NPRA:NPRC ratio at 4 weeks (Figure 7H). Although these data suggest that gWAT in β ARKnt mice may have enhanced NP responsiveness at 4 weeks, we did not observe a significant increase in UCP-1 protein expression until 16 weeks of HFD. Together, these data demonstrate that neither an increase in β_3 AR nor NP activation is sufficient to explain the enhanced gWAT UCP-1 and thermogenic activity observed in the β ARKnt mice in this study. This highlights the need for additional gWAT signaling studies and

TABLE 1 Measures of Echocardiographic Parameters From NLC and Tg β ARKnt Mice at Baseline, and 4 and 14 Weeks After HFD

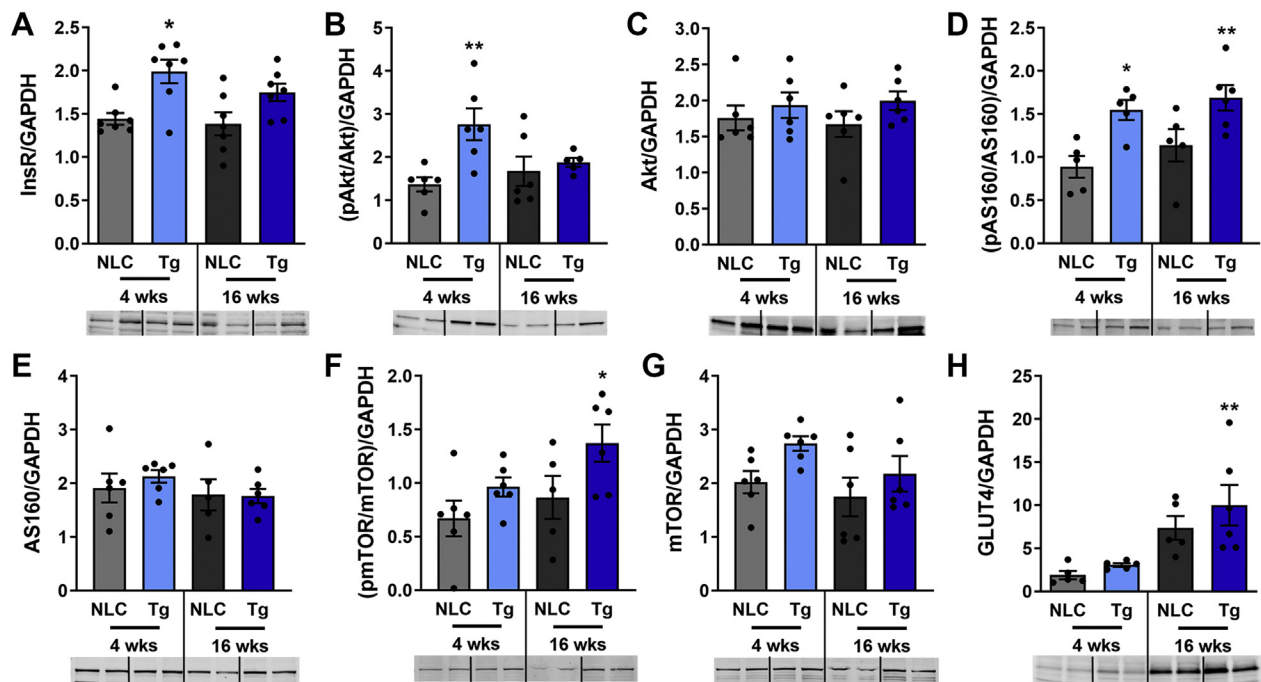
		Baseline	4 Weeks	14 Weeks
HR, beats/min	NLC	453.90 \pm 10.88	493.40 \pm 7.41	491.30 \pm 16.43
	TG	438.90 \pm 12.48	482.20 \pm 11.49 ^b	449.40 \pm 10.00 ^c
EF, %	NLC	52.42 \pm 1.29	52.33 \pm 1.99	51.87 \pm 2.16
	TG	57.72 \pm 1.60	66.77 \pm 1.23 ^{c,g}	70.20 \pm 1.9 ^{d,g}
LVPWs, mm	NLC	0.96 \pm 0.03	1.01 \pm 0.03	1.06 \pm 0.04 ^a
	TG	1.07 \pm 0.03	1.31 \pm 0.03 ^{d,g}	1.42 \pm 0.05 ^{d,g}
LVPWd, mm	NLC	0.65 \pm 0.02	0.70 \pm 0.02 ^d	0.88 \pm 0.05 ^c
	TG	0.72 \pm 0.02	0.89 \pm 0.02 ^{c,f}	0.95 \pm 0.04 ^d
LVIDs, mm	NLC	2.88 \pm 0.07	2.85 \pm 0.08	2.72 \pm 0.10
	TG	2.61 \pm 0.07 ^e	2.29 \pm 0.06 ^{b,g}	2.26 \pm 0.07 ^{c,f}
LVIDd, mm	NLC	3.91 \pm 0.06	3.87 \pm 0.06	3.68 \pm 0.08 ^a
	TG	3.72 \pm 0.06	3.59 \pm 0.07 ^e	3.73 \pm 0.10
ESV, μ L	NLC	31.94 \pm 1.75	31.24 \pm 2.19	28.30 \pm 2.81
	TG	25.11 \pm 1.57 ^e	18.16 \pm 1.26 ^{b,g}	17.65 \pm 1.31 ^{b,f}
EDV, μ L	NLC	66.74 \pm 2.30	65.12 \pm 2.44	57.69 \pm 3.17 ^a
	TG	59.01 \pm 2.13	54.41 \pm 2.59 ^e	59.98 \pm 3.98
SV, μ L	NLC	34.80 \pm 0.95	33.88 \pm 1.37	29.39 \pm 1.09
	TG	33.90 \pm 1.27	36.25 \pm 1.64	42.33 \pm 3.42 ^{c,g}

Values are mean \pm SEM. n = 11-12 per group. ^a*p* < 0.05. ^b*p* < 0.01. ^c*p* < 0.001. ^d*p* < 0.0001 by 2-way analysis of variance (ANOVA) with repeated measures and Tukey post hoc test relative to corresponding baseline. ^e*p* < 0.05. ^f*p* < 0.001. ^g*p* < 0.0001 by 2-way ANOVA with repeated measures and Bonferroni post-hoc test relative to corresponding NLC at baseline, 4 or 14 weeks post-HFD.
 EDV = end-diastolic volume; EF = ejection fraction; ESV = end-systolic volume; HR = heart rate; LVIDd = left ventricular internal diameter during diastole; LVIDs = left ventricular internal diameter during systole; LVPWd = left ventricular posterior wall thickness during diastole; LVPWs = left ventricular posterior wall thickness during systole; SV = stroke volume.

suggests there may be a noncanonical heart-to-fat pathway in these mice.

DISCUSSION

Herein, we investigated whether the enhanced cardiomyocyte AS160 signaling and reduced gWAT weight observed in our β ARKnt line would translate to cardioprotection and/or improved systemic metabolism in a mouse model of HFD-induced metabolic dysfunction. Cardiac-specific Tg β ARKnt mice exhibited equivalent weight gain over time on HFD, yet enhanced systemic glucose tolerance and insulin sensitivity, with a coordinate increase in metabolic flexibility and energy expenditure. Interrogation of the white adipose tissue phenotype revealed reduced gWAT weight and adipocyte size, and increased markers of anti-inflammation and beiging both before and after HFD stress that was not due to classical activation of the gWAT through β_3 AR or natriuretic peptides. This was accompanied by an improved brown adipose tissue morphology. More importantly, the β ARKnt mice exhibited enhanced cardiovascular function, despite no improvement in tissue remodeling, which may be again due to enhanced

FIGURE 6 Interrogation of Cardiac Insulin Signaling Pathways

Interrogation of cardiac insulin signaling pathways demonstrated enhanced phosphorylation of Akt, AS160 and mTOR suggest a distinct mechanism to beneficially regulate cardiac metabolism following HFD stress. Quantification and representative images of (A) insulin receptor (InsR), (B) phosphorylated Akt (pAkt) normalized to total Akt, (C) total Akt, (D) phosphorylated AS160 (pAS160) normalized to total AS160, (E) total AS160, (F) phosphorylated mTOR at serine 2448 (pmTOR) normalized to total mTOR, (G) total mTOR, and (H) GLUT 4 in NLC and Tg β ARKnt left ventricular tissue at 4 weeks or 16 weeks after HFD ($n = 4-7$ per group from 6-7 Western blots). All data are normalized to GAPDH within their respective blot before or after normalization to total protein levels, as appropriate. * $P < 0.05$; ** $P < 0.01$ by 1-way ANOVA with repeated measures and Tukey post hoc test relative to NLC 4 weeks. † $P < 0.05$ by one-way ANOVA with repeated measures and Tukey post hoc test relative to corresponding Tg 4 weeks or NLC 16 weeks post-HFD. Abbreviations as in Figure 1.

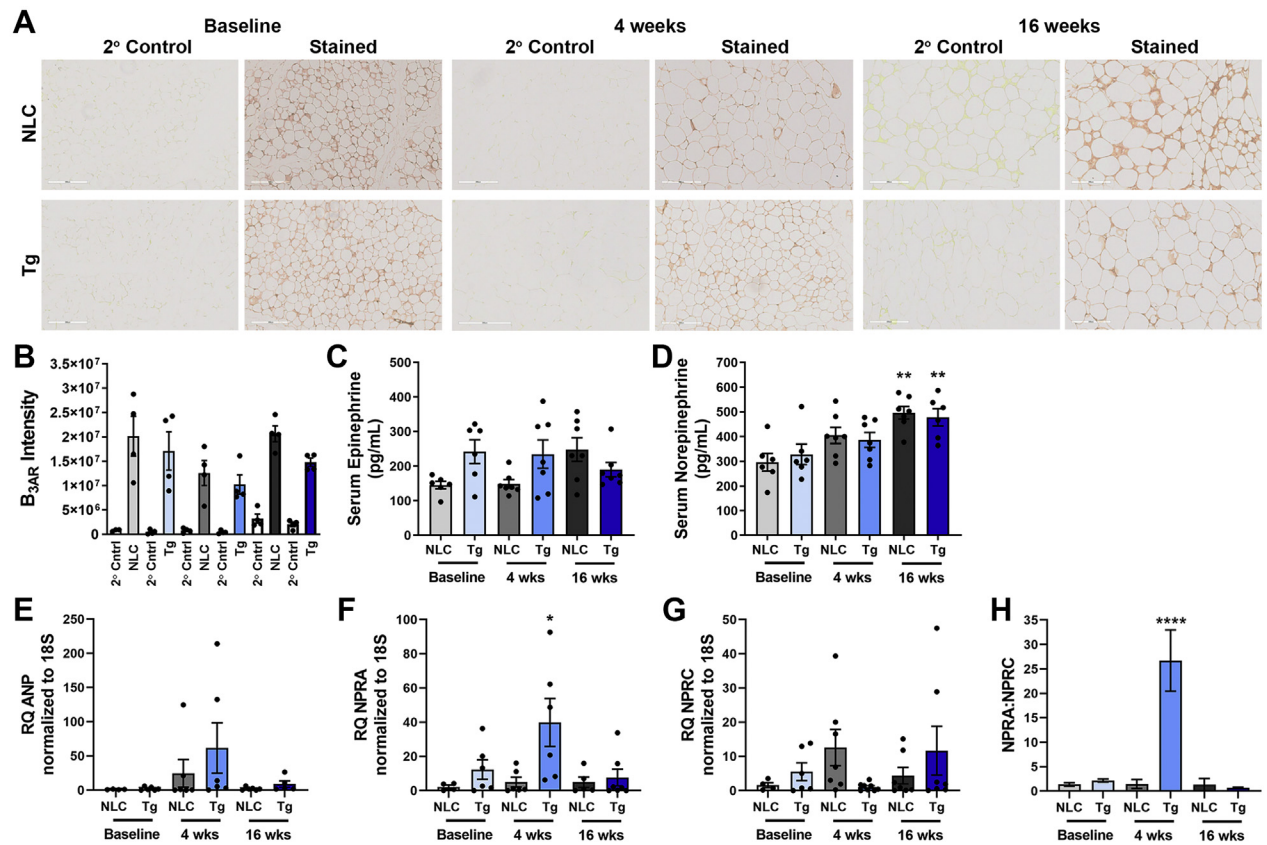
cardiovascular insulin-mediated AS160 signaling in these hearts.

The canonical role of GRK2 in regulating normal heart function through G-protein coupled receptor (GPCR) desensitization has been well established; however, in addition to this classical activity, GRK2 has been shown to display noncanonical regulatory functions in numerous cell signaling routes including mitochondrial function and apoptosis, and insulin signaling.^{8,15} Furthermore, GRK2 has been demonstrated to affect cardiac and systemic metabolic activity, though the beneficial versus detrimental effects are time and tissue dependent.^{27,41} Although overexpression of GRK2 displays resistance to HFD-induced obesity and enhanced GLUT4 levels in gWAT, cardiac-restricted expression of β ARKct negatively alters systemic metabolism and enhances the obesogenic phenotype.²⁷ Recently, our lab demonstrated that cardiac expression of β ARKnt after pressure overload positively modulates cardiac

metabolism and reduces gWAT size, in addition to its cardioprotective effects.²³ Thus, whereas increased GRK2 is detrimental for the heart and fine for the metabolic system, β ARKnt is beneficial for both, protecting the heart and reducing only the abdominal fat pad.

Insulin-sensitive tissues including adipose tissues, liver, skeletal muscle, and the heart play a crucial role in regulating systemic metabolism.^{42,43} Over the past decade, great progress has been made in interrogating the complexity of these tissues and their interactive roles in metabolism.⁴² These studies have revealed that obesity-driven insulin resistance in these tissues is the primary cause for the development of systemic dysregulation and T2D.^{42,43} During insulin resistance, normally insulin-sensitive tissues lose their response, leading to impaired glucose uptake and resulting in elevated blood glucose levels that stimulate pancreatic β cell secretion of more insulin in a detrimental feed-forward cycle.^{29,44,45} There are several

FIGURE 7 Adrenergic and Natriuretic Peptide Signaling in Tg β ARKnt Mice After HFD Stress



Despite comparable differences in β_3 AR expression, Tg β ARKnt mice exhibit an increase in NPRA mRNA levels after 4 weeks of HFD stress. (A) Representative images of β_3 AR-stained gonadal white adipose tissues (gWAT) from NLC and Tg β ARKnt mice at baseline, and 4 weeks and 16 weeks after HFD (scale bar: 222 μ m; magnification: 15 \times). (B) Quantification of β_3 AR intensity in these mice at baseline, and 4 and 16 weeks after HFD (n = 4 per group). Serum levels of (C) epinephrine and (D) norepinephrine in these groups (n = 5-7 per group). Quantification of RT-PCR data in gWAT in these mice showing fold change (RQ = 2^{- $\Delta\Delta$ C_t}) in mRNA expression of (E) ANP, (F) NPRA, (G) NPRC, and (H) NPRA:NPRC markers (n = 4-8 per group). *P < 0.05; **P < 0.01; ****P < 0.0001 by 1-way ANOVA with repeated measures and Tukey post hoc test relative to corresponding NLC baseline. Abbreviations as in Figures 1 and 3.

hypotheses regarding the mechanistic pathways responsible for insulin resistance during obesity, including adipocyte dysfunction, inflammation, hyperinsulinemia, endoplasmic reticulum stress, and mitochondrial dysfunction.⁴⁴ Although there is as of yet no unifying mechanism for insulin resistance, these mechanistic pathways are typically associated with obesity.

WAT is a complex organ that not only acts as a reservoir for energy storage, but also senses energy demands and releases adipokines to modulate other metabolic tissues.⁴³ In a high-energy state, WAT secretes adipokines such as leptin and adiponectin to regulate food intake, increase energy expenditure, and enhance insulin sensitivity and glucose metabolism.⁴⁶ Interestingly, recent studies have shown

that sustained BAT thermogenic activation leads to WAT beiging, and these brown-like adipocytes eventually produce heat via UCP-1 to improve systemic metabolism energy balance.⁴⁷ Further, this increase in gWAT UCP-1 content in mice is strongly linked to protection against diet induced obesity and systemic dysfunction.^{33,48} Although some investigators suggest that WAT beiging may induce additional improvements in energy expenditure and metabolite utilization through mechanisms independent of UCP-1, the actual relevance of WAT beiging to systemic metabolism remains unclear. Interestingly, the β ARKnt peptide elicited improved WAT activity via increased beiging and thermogenesis with no indication of altered BAT function in response to obesity. These findings reveal that cardiac β ARKnt beneficially

induces browning in gWAT, rather than BAT, to protect against HFD stress and systemic dysfunction. The mechanism by which cardiac β ARKnt increases gWAT, not BAT, UCP-1 will require further investigation. These findings suggest that although the effects of obesity on insulin-sensitive tissues is well-established, a unique link between the heart and adipose tissues via cardiometabolic modulation and/or cardiokine secretion may provide new insights for adipose and systemic dysfunction.

One caveat of this study is that we did not directly measure insulin responsiveness or metabolite uptake in WAT, BAT, liver, or skeletal muscle, so we cannot exclude the regulatory role of these tissues in the improved systemic metabolism. In *ob/ob* mice and isolated hearts of HFD mice, obesity does not impair mitochondrial fat metabolism but rather impairs insulin-stimulated glucose oxidation in a manner similar to diabetes, resulting in glucose intolerance and insulin resistance.^{49,50} Future studies could directly measure changes in glucose and fatty acid uptake into these tissues following fasting and a bolus injection of [³H]2-deoxyglucose or 2-bromopalmitate, with or without insulin stimulation, followed by tissue recovery counting.^{51,52} Comparing the heart to other metabolically active tissues would allow us to determine whether it is just the cardiac β ARKnt enhancing cardiovascular metabolism or if the heart is somehow signaling to increase insulin sensitivity and metabolite uptake in the systemic tissues as well. Our previous study demonstrated that cardiomyocytes did not undergo a switch to glucose utilization, as is often seen during cardiovascular disease and considered detrimental. Rather, they had enhanced fatty acid and glucose utilization that contributed to the increased ATP production and spare respiratory capacity.²³ Thus, these future studies would also be important to fully understand our indirect calorimetry results, particularly whether the increase in observed RER was due only to a decrease in lipid use or could be due to increase glucose utilization, or a combination effect.

Our previous study identified a novel interaction of β ARKnt with endogenous AS160 in the heart, and enhanced cardiac insulin and AS160 signaling. AS160 is expressed in multiple insulin-responsive tissues, though predominantly WAT, skeletal muscle, and the heart.⁵³ In fact, AS160 was first discovered in adipocytes, where improper Akt-dependent activation led to defective glucose uptake.⁵⁴ Patients carrying a premature stop mutation in 1 allele of AS160 (R363X), resulting in lower levels of AS160 protein and a

dominant-negative truncated variant, exhibit severe insulin resistance during puberty and post-prandial hyperinsulinemia, due to impaired insulin-stimulated GLUT4 translocation.⁵⁵ Impaired insulin-induced phosphorylation of AS160 has also been demonstrated in type 2 diabetic patient muscle, with phosphorylation and insulin sensitivity improved by endurance training.⁵⁶ Knockout models of AS160 have also demonstrated systemic insulin resistance without diabetes, wherein insulin resistance, reduced GLUT4 levels, and glucose uptake were greatest in the skeletal muscle and WAT.⁵³ In other studies, specific ablation of AS160 in skeletal muscle, adipocytes, hepatocytes, and neurons lead to tissue-specific cross-talks causing whole-body insulin resistance.^{57,58} Unfortunately, due to limitations, these mouse models cannot evaluate the cardiometabolic influence of AS160 on insulin-responsive physiological changes in glucose uptake or the metabolic flexibility and efficiency of myocytes. Further, little information is known about how disruption in AS160 signaling alters cardiac insulin resistance and metabolic function. Nonetheless, the studies point to the role of AS160 as a central node regulating glucose uptake and systemic metabolic homeostasis. The present study revealed an increase in insulin-mediated AS160 signaling in the β ARKnt hearts during acute and chronic HFD-induced metabolic stress, similar to what we previously observed during cardiac stress.²³ Importantly, though, because β ARKnt is only expressed in the hearts of these mice, the observed changes in systemic tissue function and insulin responsiveness are not due to a direct effect of β ARKnt/AS160 in those tissues but through some other means of systemic signaling. Future studies will be needed to elucidate whether AS160 plays a causative role in the beneficial effects of β ARKnt on systemic metabolism and the underlying mechanism of these effects.

Although the mechanism by which adipose tissue dysfunction contributes to cardiac pathology has been thoroughly investigated,⁴³ whether the heart can reciprocally modulate adipose tissue or other metabolically active organs remains unclear. In response to cardiac or metabolic stress, and depending upon disease stage and etiology, disrupted metabolic processes lead the heart to secrete proteins into the circulation, called cardiokines.⁵⁹ These proteins can act as autocrine (self), paracrine (adjacent cell), or endocrine (peripheral blood) factors to induce cellular responses, with endocrine actions of particular interest in seeking to understand when and how

the heart initiates communication with peripheral organs. Although our preliminary data suggest that the reduced gWAT weight and being observed in the β ARKnt mice could not be explained by enhanced β_3 AR, circulating catecholamines, or NP stimulation, future studies would be needed to exclude these processes and fully elucidate the mechanism by which cardiac β ARKnt beneficially influences the gWAT, or other metabolically active tissue, phenotype. This will include elucidating whether cardiac β ARKnt stimulates secretion of cardiokine(s) that directly act on the adipose tissue or liver. Although our data suggest cardiac-driven regulation of systemic metabolism, it may instead be an indirect effect of significant alterations in cardiomyocyte metabolism, or metabolite usage. This would still represent an as yet unknown level of interorgan sensing, or whole-body metabolite sensing, that would be worthy of investigation.

CONCLUSIONS

In summary, the present study demonstrates that cardiac-restricted expression of β ARKnt beneficially modulates abdominal fat function and systemic metabolism through improvements in insulin sensitivity and energy utilization. These findings also provide further support that cardiac β ARKnt ameliorates pathological left ventricular remodeling through direct modulation of insulin signaling pathways within cardiomyocytes and translates them into beneficial effects on systemic metabolism. The growing incidence of obesity and metabolic syndrome emphasizes the need for therapeutic interventions that improve myocardial function while simultaneously reducing abdominal fat. Therefore, a better understanding of the molecular alterations responsible for the improved adipose tissue phenotype in the β ARKnt mice may identify therapeutic targets to enhance the function of adipose tissue and systemic metabolism. Further, these studies will provide insight into cardiac regulation of systemic insulin responsiveness and may lead to new treatment modalities for cardioprotection in obesity and obesity-related metabolic syndromes.

ACKNOWLEDGMENTS The authors thank Dr Brown and his lab in the Department of Cardiovascular and Metabolic Sciences for training in the use of the Oxymax CLAMS metabolic cage setup and providing other intellectual input during these metabolic studies. The authors thank Dr Hine in the department for training them to use the EchoMRI. They also thank Dr John Peterson, Project Staff from the Imaging Core,

for his assistance in designing templates for whole-tissue histological analysis.

FUNDING SUPPORT AND AUTHOR DISCLOSURES

This work was supported by National Institutes of Health grants R00 HL132882 to Dr Schumacher and 1S10OD021561 to Dr Prasad. All other authors have reported that they have no relationships relevant to the contents of this paper to disclose.

ADDRESS FOR CORRESPONDENCE: Dr Sarah M. Schumacher, Department of Cardiovascular & Metabolic Sciences, Lerner College of Medicine, CWRU, Lerner Research Institute, NB50, Cleveland Clinic, 9500 Euclid Avenue, Cleveland, Ohio 44195, USA. E-mail: basss4@ccf.org.

PERSPECTIVES

COMPETENCY IN MEDICAL KNOWLEDGE: Heart disease remains the leading cause of death, and cardiovascular mortality rates positively correlate with the presence of diabetes and metabolic syndrome. Independent of sex, age, and developmental status of the country, the worldwide prevalence of obesity and severe obesity (body mass index ≥ 35 kg/m²) continues to progress with adverse effects on cardiovascular risk factors including plasma glucose and lipids, arterial blood pressure, inflammation, and cardiorespiratory fitness. Despite the correlation between cardiac and metabolic dysfunction, the exact mechanistic links are not fully understood. This study reveals that cardiac-restricted expression of a peptide of the GRK2 amino-terminus (β ARKnt) preserves systemic insulin responsiveness and reduces maladaptive adipose tissue remodeling despite diet-induced obesity. These data suggest that altering cardiac function may induce a clinically relevant improvement in both cardiac and systemic responses to obesity and metabolic disease.

TRANSLATIONAL OUTLOOK: In the midst of a growing recognition of the effect of adipose tissue dysfunction and adipokine imbalance on cardiovascular disease in the obese population, a less-well understood mechanism is that of the effect of cardiac metabolism and function on whole-body metabolic homeostasis. This study demonstrates that cardiac-restricted expression of a GRK2 amino-terminal peptide (β ARKnt) preserves insulin sensitivity and glucose tolerance in a model of diet-induced obesity. Moreover, cardiac β ARKnt expression protects against maladaptive adipocyte hypertrophy and adipose tissue dysfunction. Elucidating the mechanism whereby cardiac β ARKnt improves both cardiac and systemic responses to obesity will provide insight into cardiac regulation of systemic metabolic homeostasis and lead to new treatment modalities for metabolic syndrome.

REFERENCES

- Malik S, Wong ND, Franklin SS, et al. Impact of the metabolic syndrome on mortality from coronary heart disease, cardiovascular disease, and all causes in United States adults. *Circulation*. 2004;110:1245-1250.
- Saydah SH, Eberhardt MS, Loria CM, Brancati FL. Age and the burden of death attributable to diabetes in the United States. *Am J Epidemiol*. 2002;156:714-719.
- Lavie CJ, Alpert MA, Arena R, Mehra MR, Milani RV, Ventura HO. Impact of obesity and the obesity paradox on prevalence and prognosis in heart failure. *J Am Coll Cardiol HF*. 2013;1:93-102.
- Lavie CJ, McAuley PA, Church TS, Milani RV, Blair SN. Obesity and cardiovascular diseases: implications regarding fitness, fatness, and severity in the obesity paradox. *J Am Coll Cardiol*. 2014;63:1345-1354.
- Fuster JJ, Ouchi N, Gokce N, Walsh K. Obesity-induced changes in adipose tissue microenvironment and their impact on cardiovascular disease. *Circ Res*. 2016;118:1786-1807.
- Bays HE. Adiposopathy is "sick fat" a cardiovascular disease? *J Am Coll Cardiol*. 2011;57:2461-2473.
- Biddinger SB, Kahn CR. From mice to men: insights into the insulin resistance syndromes. *Annu Rev Physiol*. 2006;68:123-158.
- Ciccarelli M, Chuprun JK, Rengo G, et al. G protein-coupled receptor kinase 2 activity impairs cardiac glucose uptake and promotes insulin resistance after myocardial ischemia. *Circulation*. 2011;123:1953-1962.
- Baskin KK, Bookout AL, Olson EN. The heart-liver metabolic axis: defective communication exacerbates disease. *EMBO Mol Med*. 2014;6:436-438.
- Fujiu K, Shibata M, Nakayama Y, et al. A heart-brain-kidney network controls adaptation to cardiac stress through tissue macrophage activation. *Nat Med*. 2017;23:611-622.
- Grueter CE, van Rooij E, Johnson BA, et al. A cardiac microRNA governs systemic energy homeostasis by regulation of MED13. *Cell*. 2012;149:671-683.
- Birkenfeld AL, Boschmann M, Engeli S, et al. Atrial natriuretic peptide and adiponectin interactions in man. *PLoS One*. 2012;7:e43238.
- Collins S. A heart-adipose tissue connection in the regulation of energy metabolism. *Nat Rev Endocrinol*. 2014;10:157-163.
- Ungerer M, Bohm M, Elce JS, Erdmann E, Lohse MJ. Altered expression of beta-adrenergic receptor kinase and beta 1-adrenergic receptors in the failing human heart. *Circulation*. 1993;87:454-463.
- Pfleger J, Gross P, Johnson J, et al. G protein-coupled receptor kinase 2 contributes to impaired fatty acid metabolism in the failing heart. *J Mol Cell Cardiol*. 2018;123:108-117.
- Dzimiri N, Basco C, Moorji A, Afrane B, Al-Halees Z. Characterization of lymphocyte beta 2-adrenoceptor signaling in patients with left ventricular volume overload disease. *Clin Exp Pharmacol Physiol*. 2002;29:181-188.
- Dzimiri N, Muiya P, Andres E, Al-Halees Z. Differential functional expression of human myocardial G protein receptor kinases in left ventricular cardiac diseases. *Eur J Pharmacol*. 2004;489:167-177.
- Hata JA, Williams ML, Schroder JN, et al. Lymphocyte levels of GRK2 (betaARK1) mirror changes in the LVAD-supported failing human heart: lower GRK2 associated with improved beta-adrenergic signaling after mechanical unloading. *J Card Fail*. 2006;12:360-368.
- Mayor F Jr, Cruces-Sande M, Arcones AC, et al. G protein-coupled receptor kinase 2 (GRK2) as an integrative signalling node in the regulation of cardiovascular function and metabolic homeostasis. *Cell Signal*. 2018;41:25-32.
- Vila-Bedmar R, Garcia-Guerra L, Nieto-Vazquez I, et al. GRK2 contribution to the regulation of energy expenditure and brown fat function. *FASEB J*. 2012;26:3503-3514.
- Penela P, Murga C, Ribas C, Lafarga V, Mayor F Jr. The complex G protein-coupled receptor kinase 2 (GRK2) interactome unveils new physiopathological targets. *Br J Pharmacol*. 2010;160:821-832.
- Schumacher SM, Gao E, Cohen M, Lieu M, Chuprun JK, Koch WJ. A peptide of the RGS domain of GRK2 binds and inhibits G α (q) to suppress pathological cardiac hypertrophy and dysfunction. *Sci Signal*. 2016;9:ra30.
- Bledzka KM, Manaserh IH, Grondolsky J, et al. A peptide of the amino-terminus of GRK2 induces hypertrophy and yet elicits cardioprotection after pressure overload. *J Mol Cell Cardiol*. 2021;154:137-153.
- Surwit RS, Kuhn CM, Cochrane C, McCubbin JA, Feinglos MN. Diet-induced type II diabetes in C57BL/6J mice. *Diabetes*. 1988;37:1163-1167.
- Ahren B, Pacini G. Insufficient islet compensation to insulin resistance vs. reduced glucose effectiveness in glucose-intolerant mice. *Am J Physiol Endocrinol Metab*. 2002;283:E738-E744.
- Prpic V, Watson PM, Frampton IC, Sabol MA, Jezek GE, Gettys TW. Differential mechanisms and development of leptin resistance in A/J versus C57BL/6J mice during diet-induced obesity. *Endocrinology*. 2003;144:1155-1163.
- Woodall BP, Gresham KS, Woodall MA, et al. Alteration of myocardial GRK2 produces a global metabolic phenotype. *JCI Insight*. 2019;5(10):e123848. <https://doi.org/10.1172/jci.insight.123848>
- Ormazabal V, Nair S, Elfeky O, Aguayo C, Salomon C, Zuniga FA. Association between insulin resistance and the development of cardiovascular disease. *Cardiovasc Diabetol*. 2018;17:122.
- Manaserh IH, Maly E, Jahromi M, Chikkamenahalli L, Park J, Hill J. Insulin sensing by astrocytes is critical for normal thermogenesis and body temperature regulation. *J Endocrinol*. 2020;247:39-52.
- Ghadieh HE, Russo L, Muturi HT, et al. Hyperinsulinemia drives hepatic insulin resistance in male mice with liver-specific Ceacam1 deletion independently of lipolysis. *Metabolism*. 2019;93:33-43.
- Rosen ED, Spiegelman BM. Adipocytes as regulators of energy balance and glucose homeostasis. *Nature*. 2006;444:847-853.
- Rosen ED, Spiegelman BM. What we talk about when we talk about fat. *Cell*. 2014;156:20-44.
- Liu D, Bordicchia M, Zhang C, et al. Activation of mTORC1 is essential for beta-adrenergic stimulation of adipose browning. *J Clin Invest*. 2016;126:1704-1716.
- Heeren J, Munzberg H. Novel aspects of brown adipose tissue biology. *Endocrinol Metab Clin North Am*. 2013;42:89-107.
- Lopaschuk GD, Folmes CD, Stanley WC. Cardiac energy metabolism in obesity. *Circ Res*. 2007;101:335-347.
- Collins S, Cao W, Robidoux J. Learning new tricks from old dogs: beta-adrenergic receptors teach new lessons on firing up adipose tissue metabolism. *Mol Endocrinol*. 2004;18:2123-2131.
- Lafontan M, Berlan M. Fat cell adrenergic receptors and the control of white and brown fat cell function. *J Lipid Res*. 1993;34:1057-1091.
- Liu D, Ceddia RP, Collins S. Cardiac natriuretic peptides promote adipose 'browning' through mTOR complex-1. *Mol Metab*. 2018;9:192-198.
- Moro C, Smith SR. Natriuretic peptides: new players in energy homeostasis. *Diabetes*. 2009;58:2726-2728.
- Anand-Srivastava MB. Natriuretic peptide receptor-C signaling and regulation. *Peptides*. 2005;26:1044-1059.
- Garcia-Guerra L, Nieto-Vazquez I, Vila-Bedmar R, et al. G protein-coupled receptor kinase 2 plays a relevant role in insulin resistance and obesity. *Diabetes*. 2010;59:2407-2417.
- Kahn CR, Wang G, Lee KY. Altered adipose tissue and adipocyte function in the pathogenesis of metabolic syndrome. *J Clin Invest*. 2019;129:3990-4000.
- Longo M, Zatterale F, Naderi J, et al. Adipose tissue dysfunction as determinant of obesity-associated metabolic complications. *Int J Mol Sci*. 2019;20(9):2358. <https://doi.org/10.3390/ijms20092358>
- Ye J. Mechanisms of insulin resistance in obesity. *Front Med*. 2013;7:14-24.
- Czech MP. Insulin action and resistance in obesity and type 2 diabetes. *Nat Med*. 2017;23:804-814.
- Sun K, Kusminski CM, Scherer PE. Adipose tissue remodeling and obesity. *J Clin Invest*. 2011;121:2094-2101.

47. Wu J, Bostrom P, Sparks LM, et al. Beige adipocytes are a distinct type of thermogenic fat cell in mouse and human. *Cell*. 2012;150:366-376.
48. Kopecky J, Hodny Z, Rossmeisl M, Syrový I, Kozak LP. Reduction of dietary obesity in aP2-Ucp transgenic mice: physiology and adipose tissue distribution. *Am J Physiol*. 1996;270:E768-E775.
49. Carley AN, Severson DL. Fatty acid metabolism is enhanced in type 2 diabetic hearts. *Biochim Biophys Acta*. 2005;1734:112-126.
50. Belke DD, Larsen TS, Gibbs EM, Severson DL. Altered metabolism causes cardiac dysfunction in perfused hearts from diabetic (db/db) mice. *Am J Physiol Endocrinol Metab*. 2000;279:E1104-E1113.
51. Brown JM, Boysen MS, Chung S, et al. Conjugated linoleic acid induces human adipocyte delipidation: autocrine/paracrine regulation of MEK/ERK signaling by adipocytokines. *J Biol Chem*. 2004;279:26735-26747.
52. Brown JM, Boysen MS, Jensen SS, et al. Iso-mer-specific regulation of metabolism and PPARgamma signaling by CLA in human pre-adipocytes. *J Lipid Res*. 2003;44:1287-1300.
53. Wang HY, Ducommun S, Quan C, et al. AS160 deficiency causes whole-body insulin resistance via composite effects in multiple tissues. *Biochem J*. 2013;449:479-489.
54. Tan SX, Ng Y, Burchfield JG, et al. The Rab GTPase-activating protein TBC1D4/AS160 contains an atypical phosphotyrosine-binding domain that interacts with plasma membrane phospholipids to facilitate GLUT4 trafficking in adipocytes. *Mol Cell Biol*. 2012;32:4946-4959.
55. Dash S, Sano H, Rochford JJ, et al. A truncation mutation in TBC1D4 in a family with acanthosis nigricans and postprandial hyperinsulinemia. *Proc Natl Acad Sci U S A*. 2009;106:9350-9355.
56. Vind BF, Pehmoller C, Treebak JT, et al. Impaired insulin-induced site-specific phosphorylation of TBC1 domain family, member 4 (TBC1D4) in skeletal muscle of type 2 diabetes patients is restored by endurance exercise-training. *Diabetologia*. 2011;54:157-167.
57. Sharma M, Dey CS. AKT ISOFORMS-AS160-GLUT4: the defining axis of insulin resistance. *Rev Endocr Metab Disord*. 2021;22(4):973-986.
58. Hargett SR, Walker NN, Keller SR. Rab GAPs AS160 and Tbc1d1 play nonredundant roles in the regulation of glucose and energy homeostasis in mice. *Am J Physiol Endocrinol Metab*. 2016;310:E276-E288.
59. Dewey CM, Spittler KM, Ponce JM, Hall DD, Grueter CE. Cardiac-secreted factors as peripheral metabolic regulators and potential disease biomarkers. *J Am Heart Assoc*. 2016;5(6):e003101. <https://doi.org/10.1161/JAHA.115.003101>

KEY WORDS beiging, cardioprotection, GRK2, metabolism, obesity

APPENDIX For an expanded Methods section and supplemental figures, please see the online version of this paper.